HHS Public Access

Author manuscript

Cell Rep. Author manuscript; available in PMC 2016 July 21.

Published in final edited form as:

Cell Rep. 2015 July 21; 12(3): 449–461. doi:10.1016/j.celrep.2015.06.023.

UBE3A regulates synaptic plasticity and learning and memory by controlling SK2 channel endocytosis

Jiandong Sun[1], **Guoqi Zhu**[2], **Yan Liu**[1], **Steve Standley**[1], **Angela Ji**[1], **Rashmi Tunuguntla**[1], **Yubin Wang**[1], **Chad Claus**[1], **Lyna Luo**[1], **Michel Baudry**[1], and **Xiaoning Bi**[1]

[1] Western University of Health Sciences Pomona, CA 91766

[2] Key Laboratory of Xin'an Medicine, Ministry of Education, Anhui University of Traditional Chinese Medicine, Hefei 230038, China

Summary

Gated solely by activity-induced changes in intracellular calcium, small conductance potassium channels (SKs) are critical for a variety of functions in the CNS, from learning and memory to rhythmic activity and sleep. While there is a wealth of information on SK2 gating, kinetics and Ca^{2+} sensitivity, little is known regarding the regulation of SK2 subcellular localization. We report here that synaptic SK2 levels are regulated by the E3 ubiquitin ligase UBE3A, whose deficiency results in Angelman syndrome and over-expression in increased risk of autistic spectrum disorder. UBE3A directly ubiquitinates SK2 in the C-terminal domain, which facilitates endocytosis. In UBE3A-deficient mice, increased postsynaptic SK2 levels result in decreased NMDA receptor activation, thereby impairing hippocampal long-term synaptic plasticity. Impairments in both synaptic plasticity and fear conditioning memory in UBE3A-deficient mice are significantly ameliorated by blocking SK2. These results elucidate a mechanism by which UBE3A directly influences cognitive function.

Introduction

Information processing in central nervous system (CNS) circuits depends on synaptic activity. In particular, synaptic transmission is modulated by different small conductance calcium-activated potassium channels (SKs), which either contribute to the afterhyperpolarization that follows an action potential or facilitate repolarization following

Address Correspondence to: Xiaoning Bi College of Osteopathic Medicine of the Pacific Western University of Health Sciences 701 E. 2nd St. Pomona, CA 91766 Tel: 909-469-5487 xbi@westernu.edu.

Author Contributions:

JS, GZ, YL performed most of the experiments, and prepared the figures.
SS, AJ, RT prepared constructs used in the experiments.
YL, CC performed fear-conditioning experiments.
YW performed some immunofluorescent experiments.
LL performed the docking experiment.
MB worked on the figures and wrote the manuscript.
XB directed the research, worked on the figures and wrote the manuscript.

excitatory postsynaptic potentials (EPSPs). SKs participate in various CNS functions, from regulating neuronal intrinsic excitability to network rhythmic activity and higher brain functions (Adelman et al., 2012; Colgin et al., 2005; Ohtsuki et al., 2012). In hippocampal CA1 pyramidal neurons, synaptic SK2s are opened upon N-methyl-D-aspartate (NMDA) receptor activation and repolarize the membrane, thereby terminating NMDA receptor function (Ngo-Anh et al., 2005). This local feedback loop between NMDARs and SK2s has been proposed to play a critical role in regulating neuronal excitability and in controlling the threshold for induction of long-term potentiation (LTP) (Hammond et al., 2006; Lin et al., 2008). LTP induction also regulates synaptic SK2 expression, as it triggers endocytosis of synaptic SK2s (Lin et al., 2008).

Accumulating evidence indicates that a number of postsynaptic proteins are ubiquitinated in an activity-dependent manner (Colledge et al., 2003; Ehlers, 2003; Guo and Wang, 2007; Patrick et al., 2003). Ubiquitination consists of modifying proteins through E3 ligase-mediated ubiquitin attachment (Komander et al., 2009). One of the E3 ligases, UBE3A, is critical for normal brain function (Huibregtse et al., 1995) since its deficiency causes Angelman syndrome (AS) (Williams et al., 1990), while its over-expression is linked to increased risk of autistic spectrum disorder (Cook et al., 1997). However, to date very few neuronal substrates of UBE3A have been identified. The current study provides evidence that UBE3A directly ubiquitinates the C-terminal domain of SK2, thereby facilitating its internalization. Deficiency in this regulation accounts for impairments in LTP and learning and memory found in UBE3A-deficient mice.

Results

Synaptic SK2 levels are increased in hippocampus of UBE3A-deficient mice

Previous research from several groups, including our own, has shown that LTP is impaired in maternal UBE3A-deficient (AS) mice (Baudry et al., 2012; Jiang et al., 1998; van Woerden et al., 2007). We hypothesized that UBE3A may directly regulate synaptic SK2 expression and that its deficiency could contribute to LTP impairment. Western blot analysis of proteins from different hippocampal subcellular fractions (Figure S1A,B) showed that SK2 levels were significantly higher in crude synaptosomal (P2, Figure 1A), and PSD-enriched (P3, Figure 1B) fractions of AS mice than in those from wild-type (WT) mice. SK2 levels in whole hippocampal homogenates were not significantly different between WT and AS mice (Figure S1C). Immunofluorescent staining showed that the highest levels of SK2 expression in hippocampal CA1 region were in cell bodies and dendrites of pyramidal neurons (Figure 1C; Figure S1E). High magnification examination revealed that SK2-immunoreactive puncta were distributed along apical dendrites and were partially co-localized with PSD95- (Figure 1C) and synaptophysin-immunopositive profiles (Figure S1E). Quantitative analysis showed that the number of SK2-immunopositive puncta was markedly increased in AS mice (Figure 1D). The percentage of puncta dually stained with SK2 and PSD95 (Figure 1D) or SK2 and synaptophysin (Figure S1F) was also significantly increased in AS mice. There was no significant difference in the overall number of PSD95-immunopositive puncta between AS and WT mice (Figure S1D).

Reduced SK2 protein ubiquitination in hippocampus of AS mice

We next determined whether the increase in synaptic SK2 levels in AS mice was due to the lack of UBE3A-mediated ubiquitination. Immunofluorescent staining showed that UBE3A and SK2 were co-localized in puncta along apical dendrites of CA1 pyramidal neurons (Figure 2A) and dendrites of cultured hippocampal neurons from WT mice (Figure S2A). Immunoprecipitation experiments showed that SK2 co-immunoprecipitated with UBE3A (upper panel in Figure 2B) and UBE3A co-immunoprecipitated with SK2 (lower panel in Figure 2B). Furthermore, the amount of ubiquitinated proteins in SK2 antibody pull-down samples from AS mice was decreased, as compared to that in WT mice (arrows in Figure 2C). Immunoprecipitation of SK2 by SK2 antibody and ubiquitination of UBE3A were also determined (Figures S2B and S2C). Immunoprecipitation performed under denaturing conditions confirmed that SK2 was ubiquitinated and its ubiquitination reduced in AS mice, as compared to WT mice (arrows in Figure 2D).

UBE3A ubiquitinates SK2

To determine whether UBE3A could ubiquitinate SK2 *in vitro,* we first incubated a purified GST-SK2 C-terminal domain (SK2-C) with ubiquitin, E1, E2, and ATP in the presence or absence of recombinant UBE3A. Under these conditions, UBE3A markedly increased SK2-C ubiquitination (Figure 3A). The presence of UBE3A and SK2-C was verified by Western blots (Figures 3A and S3A).

UBE3A-mediated SK2-C ubiquitination was then confirmed using COS-1 cells, transfected with a chimeric construct (Tac-SK2), containing the N-terminal and transmembrane domain of Tac, a constitutively expressed membrane protein (Bonifacino et al., 1990), and the SK2 C-terminus. Tac chimeric constructs have been widely used to study membrane protein trafficking (Mu et al., 2003; Standley et al., 2000). Since COS-1 cells express endogenous UBE3A, we determined the effect of siRNA-mediated knock-down of UBE3A on SK2-C ubiquitination using His-ubiquitin pull down assay. COS-1 cells were first incubated with either UBE3A siRNA or a scrambled control siRNA, followed by transfection with Tac-SK2-C and His-ubiquitin. SK2-C ubiquitination was moderately reduced (30 ± 1% reduction in UBE3A siRNA-treated, as compared to control siRNA-treated; $p<0.001$, n=3) following UBE3A siRNA treatment (Figure 3B, lower panel), to an extent matching that of UBE3A reduction (Figure 3B, upper panel; 33 ± 4%; $p<0.01$, n=3). In contrast, overall protein ubiquitination was not affected (Figure S3B). We repeated the experiments with full-length SK2 (SK2-FL) and obtained similar results (Figure S3C). Thus, results from directubiquitination assay and His-ubiquitin pull-down analysis showed that SK2 is ubiquitinated in its C-terminus by UBE3A.

Lysine residues K506, K514 and K550 in SK2 C-terminal domain are critical for UBE3A-mediated ubiquitination

Multiple lysine residues are present in SK2 C-terminus, with several in the calmodulin-binding domain (CaMBD; Figure S3D). Since calmodulin is constitutively bound to CaMBD, we targeted the three lysine residues after the CaMBD (Figure 3C). Of note, *in silico* molecular docking showed that K506 and K514, which are present in the crystal structure of SK2 C-terminal helix, are facing the binding grove of UBE3A where C604,

C737, and the catalytic C820 are located (Figure 3D). We simultaneously mutated residues K506, K514 and K550 to alanine (ΔK) in Tac-SK2-C and co-transfected this construct in COS-1 cells with either wild-type UBE3A (UBE3A) or its inactive form UBE3A-C833A (Kumar et al., 1999) (referred to as ΔUBE3A hereafter), to determine whether these mutations affected SK2-C ubiquitination, and whether ubiquitination was also influenced by the amount of functional UBE3A. Tac-SK2-C co-immunoprecipitated with UBE3A, and much less with ΔUBE3A (Figure S3E), suggesting that interaction between functional UBE3A and SK2 C-terminus is involved in SK2 ubiquitination. The His-ubiquitin pull-down assay showed that co-transfection with UBE3A, but not ΔUBE3A, resulted in massive SK2-C ubiquitination, which was significantly reduced by K-A mutation (84% ± 5% reduction compared to UBE3A/Tac-SK2-C group; $p<0.001$, n=3)(Figure 3E, lower panel). Again, overall protein ubiquitination was not affected (Figure S3F). These results confirmed that SK2s are ubiquitinated by UBE3A at K506/K514/K550 in the C-terminal domain.

To test whether these lysine residues are also involved in UBE3A-mediated ubiquitination *in vivo*, we synthesized two short peptides around K550 (PM101, and PM102, see Experimental Procedures). We first tested whether these peptides could disrupt the interaction between SK2 and UBE3A in P2 fractions of hippocampus from WT mice. Immunoprecipitation experiments showed that the amount of SK2 in UBE3A antibody pull-down products was decreased by incubation with peptides PM101 and PM102 at 50 μM (Figure 3F). Immunoprecipitation of UBE3A by UBE3A antibody was also determined (Figure 3F). To allow for efficient delivery of the peptide across the blood-brain barrier, we conjugated PM101 to the cell membrane transduction domain of HIV-1 Tat protein (TAT-101). It is well established that peptides/proteins that are fused to TAT are rapidly and efficiently introduced into live tissues when systemically administered into intact animals, while retaining their biological activity (Rapoport and Lorberboum-Galski, 2009; Xu et al., 2007). Four-month-old WT mice were injected with either control TAT or TAT-101 (i.p., 50 mg/kg), and hippocampi collected 2 h later. Western blot results showed that SK2 levels in P2 fractions were significantly increased following TAT-101 treatment (11 ± 3%; $p<0.01$, n=4), as compared to TAT control (Figure 3G). Immunoprecipitation performed under denaturing conditions confirmed that SK2 ubiquitination was also reduced in TAT-101-treated mice (30 ± 3%, $p<0.001$; n=3) as compared to control TAT-treated mice (arrows in Figure 3G). These results indicate that sequences around K550 in SK2 C-terminal domain are critical both for interaction with and ubiquitination by UBE3A *in vivo*.

UBE3A-mediated regulation of SK2 surface expression and endocytosis depends on K506/ K514/ K550

To further understand the role of UBE3A-mediated SK2 ubiquitination, we analyzed SK2 surface expression and endocytosis first in COS-1 cells. Tac-SK2 surface expression, detected with a Tac-specific antibody, was significantly reduced following co-transfection with UBE3A, but was markedly increased following ΔUBE3A co-transfection (Figures 4A and 4B left panels; Figure S4A). In contrast, co-transfection with either UBE3A or ΔUBE3A did not affect surface expression of a similar construct consisting of Tac and the C-terminal domain of the AMPA receptor subunit, GluA2 (Tac-GluA2; Figure S4B). Results similar to those obtained with Tac-SK2 were obtained with full-length SK2 (Figure S4C). The effects

of UBE3A and/or ΔUBE3A on Tac-SK2 surface expression were also confirmed by Western blots from cell membrane fractions, although co-transfection of Tac-SK2 with UBE3A or ΔUBE3A did not significantly alter SK2 levels in whole homogenates (Figure S4D). K-A mutation at K506/K514/K550 (ΔK) significantly increased surface expression and eliminated the effect of UBE3A (Figure 4A, right panels; 4B, left panel). In endocytosis assays, UBE3A significantly increased, while ΔUBE3A significantly reduced, Tac-SK2 internalization (Figure 4A, left panels; 4B, right panel; Figure S4E). K-A mutation significantly reduced SK2 endocytosis and eliminated the effect of UBE3A (Figures 4A and 4B, right panels). Similar results were obtained when lysine residues K506/K514/K550 were changed to arginine (ΔK2; Figure S4E). These results suggest that UBE3A facilitates SK2 endocytosis, possibly by ubiquitination of K506/K514/K550 residues.

To determine whether UBE3A-mediated regulation of SK2 surface expression and endocytosis in COS-1 cells also occurred in neurons, we cultured hippocampal neurons from AS and WT embryos. We first confirmed that SK2 levels were higher in membrane fractions from cultured hippocampal neurons of AS mice, as compared to WT mice (Figure 4C). We then performed biotinylation assay to detect surface-expressed and internalized SK2s in cultured hippocampal neurons. The results showed that levels of membrane-associated SK2s were significantly higher in AS neurons than in WT neurons (Figure 4D). While significant amounts of SK2s were detected in the endocytotic fraction from WT neurons, SK2s were barely detectable in the similar fraction from AS mice neurons (Figure 4D). In contrast, GluA1 was detectable in the endocytotic fraction from both WT and AS mice (Figure 4D). These results reveal a specific UBE3A-dependent regulation of SK2 endocytosis in hippocampal neurons.

Increased SK2s result in synaptic plasticity impairment and decreased NMDAR function in AS mice

To determine whether changes in SK2 synaptic expression contributed to LTP impairment in AS mice, we determined the effects of apamin, a selective SK2 blocker, on LTP in acute hippocampal slices. As previously reported, theta-burst stimulation (TBS) induced LTP in field CA1 of hippocampal slices in WT mice, whereas it only elicited transient facilitation in AS mice (Figure 5A,B; red trace). Following pre-incubation of hippocampal slices from AS mice with apamin (20 nM), TBS-elicited LTP was identical to that in WT mice (Figure 5A,B; blue trace). Apamin at this concentration did not affect TBS-induced LTP in slices from WT mice (Figure 5A,B; pink trace), nor did it affect baseline synaptic responses or responses in a control pathway (Figure 5A,B, and Figure S5A) or paired-pulse facilitation (Figure S5B) in slices from either WT or AS mice.

Like LTP, long-term depression (LTD) of synaptic transmission is also generally assumed to be involved in learning and memory. We therefore determined whether LTD was altered in AS mice. Low frequency stimulation (LFS; 1 Hz, 15 min) of the Schaffer collaterals in hippocampal slices from 3 month-old WT mice induced a transient synaptic depression, and synaptic responses slowly returned to baseline levels (white circle in the upper panel of Figure 5C), a result consistent with the literature (Dudek and Bear, 1993). However, the same protocol induced sustained LTD in slices from 3 month-old AS mice (red circle in

upper panel of Figure 5C). Apamin (20 nM) pre-treatment significantly reduced LTD in AS mice (blue in the upper panel in Figure 5C,D), and did not affect responses to low frequency stimulation in slices from WT mice. Since induction of both LTP and LTD at Schaffer collateral–CA1 synapses is NMDAR-dependent and since SK2-mediated hyperpolarization inhibits NMDAR-channel opening, we analyzed the effect of apamin treatment on NMDAR-mediated synaptic responses ($_{N}$fEPSP$_{S}$). $_{N}$fEPSPs were isolated by bath application of a Mg^{2+}-free ACSF containing 6-cyano-7-nitroquinoxaline-2,3-dione (CNQX; 10 μM) to block AMPA receptor-mediated synaptic transmission. The NMDAR antagonist, AP5, was used to verify that $_{N}$fEPSPs were mediated by NMDARs under these conditions (Figure 5E). $_{N}$fEPSP amplitudes were significantly lower in AS mice, as compared to WT mice, and this decrease was reversed by apamin application (Figure 5F,G and Figure S5C), suggesting that SK2 imposes a stronger inhibition of NMDAR in AS than in WT mice. At this concentration, apamin did not significantly increase $_{N}$fEPSP in WT mice (Figure 5F,G). AP5 pre-treatment also significantly reduced LTD in AS mice (Figure S5D), suggesting that the enhanced LTD in AS mice is also NMDAR-dependent.

To confirm that increased SK2 activity was due to the lack of UBE3A-mediated regulation, we determined the effect of the TAT-101 peptide on LTP induction in WT mice. Hippocampal slices were prepared 2 h after administration of either control TAT or TAT-101 peptide (i.p., 50 mg/kg). In hippocampal slices from TAT-101-treated mice, TBS only induced a transient enhancement in synaptic responses, as found in slices from AS mice. In contrast, LTP was intact in hippocampal slices from control TAT-treated mice (Figure 5H,I).

We previously showed that LTP impairment in AS mice was associated with reduced actin polymerization following TBS application (Baudry et al., 2012). Therefore, we determined the effect of apamin application on TBS-induced actin polymerization using Alexa 568-conjugated phalloidin, which selectively binds to filamentous actin (F-actin). TBS elicited a clear increase in the number of F-actin-positive puncta in WT slices, but not in AS slices. Apamin pre-treatment markedly enhanced TBS-induced actin polymerization in AS slices (Figure S6).

Increased SK2s alter TBS-induced LTP properties in AS mice

Recent studies have revealed that TBS-induced LTP is followed by a refractory period (about 1 h) during which another TBS cannot enhance LTP magnitude, while multiple TBS trains separated by longer time intervals are able to increase LTP magnitude (Kramar et al., 2012). This LTP property was tested in hippocampal slices from AS mice by applying a second TBS (TBS2) train at 10, 45, or 60 min after the first TBS (TBS1). As previously reported (Lynch et al., 2013), TBS2 applied 10 min (Figure 6B) post TBS1 in WT hippocampal slices failed to further enhance LTP magnitude, while after 60 min (Figure 6A) TBS2 significantly increased LTP magnitude. In contrast, TBS2 applied at 10 min (Figure 6B) or 45 min (Figures S7A and S7B) after TBS1 in AS hippocampal slices significantly enhanced LTP magnitude to a level comparable to that found in WT mice. In addition, when applied 60 min (Figure 6A) after TBS1, TBS2 failed to significantly increase LTP.

Quantitative image analysis showed that TBS1 stimulation induced a significant reduction in the percentage of SK2-immunopositive synapses in WT mice, a result in good agreement with a previous study (Lin et al., 2008). In AS mice, TBS1, although unable to induce LTP, produced a similar reduction in the percentage of SK2-immunopositive synapses, suggesting that TBS1-elicited SK2 internalization enables TBS2 to induce LTP shortly after TBS1 (Figure 6D,E). This idea was further supported by the fact that following pre-incubation with apamin in AS slices, TBS2 applied 10 min after TBS1 did not further enhance LTP (Figure 6C).

Treatment with apamin improves learning and memory performance of AS mice in the fear-conditioning paradigm

To determine whether apamin could also reverse impairment in hippocampus-dependent learning in AS mice, we used the fear conditioning paradigm. AS and WT mice were injected with apamin (0.4 mg/kg, i.p.) 30 min before the training session, as previously reported (Vick et al., 2010). AS mice were impaired in context-dependent fear-conditioning and tone test, and apamin treatment significantly enhanced learning performance in AS mice (Figure 7). Under our experimental conditions (3 conditioned stimuli (CS) paired with 3 unconditioned stimuli (US)), apamin treatment did not affect learning in WT mice. Additionally, there was no difference in freezing time in the pre-conditioning period, during training, or before tone application in the testing period between all experimental groups (Figure S7C).

Discussion

Our results indicate that UBE3A-mediated regulation of synaptic SK2s plays critical roles in synaptic plasticity and learning and memory. SK2 and UBE3A were co-localized in dendrites and spines of hippocampal pyramidal neurons and lack of UBE3A resulted in increased synaptic SK2 levels and decreased SK2 ubiquitination. SK2 was ubiquitinated by UBE3A at residues K506/K514/K550 in its C-terminal domain, resulting in SK2 internalization. Both the interaction between SK2 and UBE3A and SK2 ubiquitination were significantly reduced by small peptides that comprise the SK2 C-terminal sequence around residue K550. Electrophysiological studies revealed that increased SK2 levels imposed a tonic inhibition of NMDARs, accounting for impairments in TBS-induced LTP and actin polymerization in hippocampal slices from AS mice. The interaction-disrupting peptide TAT-101 produced LTP impairment in slices from WT mice, similar to that observed in AS mice. *In vivo* experiments demonstrated that increased synaptic SK2 levels also contributed to learning and memory deficits in the fear-conditioning paradigm. Together, these results not only indicate that SK2 is a substrate of UBE3A, but also reveal a mechanism by which UBE3A regulates synaptic plasticity and cognitive functions.

UBE3A ubiquitinates SK2s in their C-terminal domain resulting in their endocytosis

Several synaptic proteins are regulated by the ubiquitin-proteasome system (see (Lin and Man, 2013; Mabb and Ehlers, 2010) for recent reviews). For instance, PSD-95 is ubiquitinated by the E3 ligase Mdm2 leading to subsequent degradation by proteasomes in response to NMDA receptor activation (Colledge et al., 2003). PSD-95 ubiquitination also

results in increased AMPAR internalization, possibly through a non-proteolytic function, i.e., by interacting with and enhancing clathrin-dependent endocytosis (Bianchetta et al., 2011). Both NMDARs and AMPARs are also modified by protein ubiquitination; the NMDAR subunit GluN2B is ubiquitinated by the RING family E3 ligase Mib2 (Jurd et al., 2008), the AMPAR subunit GluA1 by Nedd4 (Lin et al., 2011), and GluA2 by an undefined E3 ligase (Lussier et al., 2011). Our results add to this list another member of postsynaptic proteins by showing that UBE3A ubiquitinates SK2 in its C-terminal domain, on lysine residues K506, K514, and K550. Mutations of these lysine residues to either alanine or arginine not only reduced SK2 channel endocytosis and increased their surface expression, but also eliminated UBE3A-mediated SK2 ubiquitination and endocytosis. Finally, the endocytosis-biotinylation assay showed that, while SK2 was detectable in both cell membrane and endocytotic fractions in neurons cultured from WT mice, it was only observed in cell membrane fractions in neurons from AS mice, suggesting that UBE3A deficiency impairs tonic SK2 endocytosis. The reduction in SK2 endocytosis could account for the increased SK2 levels in crude synaptosomal and PSD fractions found in hippocampus of AS mice.

Roles of UBE3A-mediated SK2 regulation in synaptic plasticity

We previously reported that a semi-chronic treatment with an AMPA receptor positive regulator, CX929, reversed LTP impairment in AS mice, possibly due to increased BDNF production. In the current study we showed that acute apamin application in hippocampal slices was able to restore TBS-induced LTP in AS mice. BDNF has been shown to facilitate NMDAR-mediated LTP, and, as we discussed, apamin treatment also increases NMDAR activity. Thus, CX929 and apamin treatments converge on NMDARs and possibly on downstream signaling pathways as well, since both CX929 treatment and apamin application were able to restore actin polymerization in dendritic spines following LTP induction. We therefore argue that LTP impairment in AS mice takes place at the induction phase, possibly due to insufficient NMDAR activation, and we postulate that any manipulation that enhances LTP induction could be beneficial to re-establish normal synaptic plasticity in AS mice. In addition, treatments bypassing the induction stage and directly activating downstream signaling cascades, such as increasing CaMKII activity (van Woerden et al., 2007) or promoting cytoskeletal remodeling (Baudry and Bi, 2013; Lynch et al., 2008) could be beneficial as well.

Recently, a series of studies have revealed that LTP has a refractory period lasting about 1 h after TBS (Lynch et al., 2013). We recently found that two different isoforms of the calcium-activated protease, calpain, play a critical role in LTP induction and the initiation of the refractory period (Wang et al., 2014). These findings provide a biological basis for the widely recognized phenomenon that new information is better retained with spaced-trial learning than with massed-trial learning (Benjamin and Tullis, 2010). In the present study, we found that at intervals ≤45 min, TBS2 was able to induce LTP in AS mice, suggesting that a short lasting process triggered by TBS1 was sufficient for facilitating LTP induction in AS mice. Since TBS2 delivered at 10 min interval did not further enhance LTP in apamin pre-treated slices, it is possible that removal of SK2 channels by TBS1 contributes, at least partly, to the reinstatement of LTP by TBS2 delivered shortly after TBS1 in hippocampal

slices from AS mice. Our immunofluorescence results support the notion that TBS1 induces SK2 internalization. Lin et al. also proposed that LTP-induced SK2 internalization depended on PKA-mediated phosphorylation and that direct SK2 phosphorylation in the C-terminal domain may initiate its endocytosis (Lin et al., 2008; Ren et al., 2006). Whether TBS1-induced SK2 removal in AS mice also depends on PKA activation and whether this process interacts with UBE3A-mediated SK2 ubiquitination are currently under investigation.

LTD has been reported to be impaired in layer 2/3 synapses in visual cortex in adult AS mice, although LTD is reliably induced in these synapses in adult WT mice (Yashiro et al., 2009). In contrast, LTD is difficult to be reliably induced in adult hippocampus (Dudek and Bear, 1993), and our results showed that this is the case in adult WT mice. However, stable LTD was induced in hippocampal slices from AS mice, which was blocked by apamin application. These results suggest that SK2 upregulation in hippocampal CA1 synapses could be responsible for LTD induction in adult AS mice. A recent study reported that mGlu5 receptor-mediated LTD was also enhanced in AS mice (Pignatelli et al., 2014). Of notice, mGlu5 receptors and SK2s have been shown to form a reciprocally regulating complex (Garcia-Negredo et al., 2014). Thus, it is possible that increased synaptic SK2 levels contribute to mGlu5 receptor-mediated LTD enhancement, and this question will be investigated in future studies.

Role of UBE3A-mediated regulation of SK2s in learning and memory

Previous studies, including our own, showed that, compared with their WT littermates, AS mice exhibit a clear deficit in context-dependent fear conditioning (Baudry et al., 2012; Jiang et al., 1998; van Woerden et al., 2007). We previously showed that a semi-chronic treatment with CX929 reversed the behavioral deficit and re-established normal levels of freezing in response to context and cue (Baudry et al., 2012). Manipulations of SK2 activity have been shown to influence learning performance in various paradigms (Deschaux et al., 1997; McKay et al., 2012; Stackman et al., 2002). A recent study showed that apamin enhanced contextual fear memory in WT mice conditioned with one CS-US pairing protocol, but not with three CS-US pairings (Vick et al., 2010). In the present study, we used three CS-US pairing protocol, and under this condition, apamin had no effect on fear-conditioning learning in WT mice, but significantly improved both context- and cue-dependent learning in AS mice. These results support our hypothesis that, in AS mice, increased levels of synaptic SK2s are responsible for hippocampal-dependent learning deficit. In summary, our results suggest that synaptic SK2 endocytosis is directly regulated by UBE3A-mediated ubiquitination and that this regulation is critically involved in synaptic plasticity and learning performance, while defects in this regulation could contribute to intellectual disability, as seen in Angelman syndrome.

Experimental Procedures

Mice

Animal experiments were conducted with protocols approved by the local Institutional Animal Care and Use Committee. Original UBE3A mutant (AS) mice were obtained from The Jackson Laboratory, strain 129-Ube3a$^{tm1Alb/J}$, and a breeding colony was established as

previously described (Baudry et al., 2012). In all experiments, male AS mice and wild-type (WT) littermates between 2–4 months were used.

Hippocampal Neuronal Cultures

Hippocampal neurons were prepared from E18 mouse embryos, bred with UBE3A$^{m-/p+}$ female and male mice, as described (Qin et al., 2009).

Cell Lines

COS-1 cells (ATCC) were grown in DMEM supplemented with 10% (vol/vol) fetal bovine serum (FBS) (Invitrogen).

DNA Constructs, Transfection, Antibodies, and Peptides

For transient expression, cells were transfected with the respective constructs and/or small interfering RNA (siRNA) by lipofection (Lipofectamine 2000; Invitrogen).

Details of DNA constructs, and antibodies can be found in Supplemental Experimental Procedures.

The following peptides were synthesized by ABI Scientific Inc: PM101 (NYDKHV), PM102 (MENYDKHVSYN), TAT (YGRKKRRQRRR), and TAT-101 (YGRKKRRQRRRNYDKHV).

Subcellular Fractionation and Western Blot Analysis

Fractionation methods were modified from those of Smith et al. (Smith et al., 2006), to yield P2 and P3 fractions relatively enriched in postsynaptic density fractions (PSDs). Western blots were performed according to published protocols (Sun et al., 2015), with IRDye secondary antibodies and detected with the Odyssey® imaging system.

Immunoprecipitation and Denaturing Immunoprecipitation

Immunoprecipitation was performed by incubating hippocampal P2 fractions with appropriate antibodies and agarose beads following standard procedures. For SK2 immunoprecipitation under denaturing conditions, P2 pellets were heated in denaturing lysis buffer, diluted in ice-cold non-denaturing lysis buffer, and then incubated with antibodies coupled to protein A/G Agarose beads.

In Vitro Ubiquitination Assay

GST-SK2 proteins containing the whole SK2 C-terminus were expressed in *E. coli* BL21 (DE3) and purified as previously described (Ren et al., 2006). The E6AP (UBE3A) Ubiquitin Ligase Kit (Boston Biochem) containing E1 and E2 enzyme (UBE2D3), His_6-UBE3A, ubiquitin, Mg^{2+}-ATP, and reaction buffer was used. For negative control reactions, ATP was omitted. Three independent experiments were performed.

His-ubiquitin Pull-down Assay

COS-1 cells were transfected with His-ubiquitin plus Tac-SK2 or ΔK, and HA-UBE3A or HAUBE3A C833A constructs, or UBE3A or control siRNA. Twenty-four h after transfection, cells were lysed, and His-ubiquitin-conjugated proteins were purified as described (Xirodimas et al., 2001), with minor modifications.

In Silico Molecular Docking

In silico molecular docking was performed between the crystal structure of SK2 C-terminal helix (PDB ID 2PNV, chain A 488 to 526) (Kim et al., 2008) and the crystal structure of UBE3A (PDB ID 1D5F) (Huang et al., 1999). Patchdock (Duhovny D, 2002; Schneidman-Duhovny et al., 2005) was used for docking.

Endocytosis Assay of Tac-SK2 in COS-1 Cells

Analysis of Tac-SK2 internalization was performed as previously reported (Roche et al., 2001; Standley et al., 2000) and detailed in Supplemental Experimental Procedures. In brief, cultured COS-1 cells were incubated with Tac7G7 antibodies on ice, antibodies bound to Tac-SK2 were allowed to be internalized, and internalized Tac-SK2 and surface-expressed Tac-SK2 were visualized by using two different fluorophore-conjugated secondary antibodies.

Image Analysis and Quantification

Images were acquired using a Nikon C1 confocal laser-scanning microscope. Acquisition parameters were kept identical among different experimental groups. All immunostaining studies were performed in 3-5 independent experiments. Tac-SK2 surface expression and internalization were analyzed using ImageJ (NIH).

Neuronal Biotinylation Assay

Neuronal biotinylation assay was performed as previously reported (Roche et al., 2001) and detailed in Supplemental Experimental Procedures. In brief, cultured hippocampal neurons were incubated with sulfo-NHS-SS-biotin (Pierce) on ice, biotinylated proteins were either precipitated with NeutrAvidin Agarose (Pierce), or allowed to be internalized, and precipitated after the remaining surface biotin was stripped.

Acute Hippocampal Slice Preparation, Electrophysiology, and Phalloidin Staining

Acute slice preparation, recordings, and phalloidin staining of F-actin were performed as previously described (Baudry et al., 2012; Wang et al., 2014).

Immunofluorescence of Brain Tissue Sections

For immunofluorescence, brain sections (25 μm) were processed as previously described (Sun et al., 2015; Wang et al., 2014).

Fear Conditioning

Male AS and wild-type mice were subjected to fear conditioning testing as described in Supplemental Experimental Procedures. On training day, mice were injected

intraperitoneally (i.p.) with apamin (0.4 mg/kg) 30 min before training. Training was conducted in a fear-conditioning chamber (H10-11M-TC, Coulbourn Instruments) and behavior was recorded with the Freezeframe software and analyzed with Freezeview software (Coulbourn Instruments).

Statistical Analysis

Error bars indicate standard error of the means. To compute p values, unpaired Student's t test, Kolmogorov-Smirnov test, and one- or two-way ANOVA with Newman-Keuls or Bonferroni post-test were used, as indicated in figure legends.

Supplementary Material

Refer to Web version on PubMed Central for supplementary material.

Acknowledgements

The authors are grateful to Dr. Gary Lynch for his insightful comments and would like to thank Ms. Stephanie Moreno, Mr. Erik Lee and Mr. Omar Abouelnasr for helping maintaning the mouse colonies, Dr. Guanghong Liao, Mr. Max Zhvanetsky, Mr. Neema Baudry, Ms. Zhuangjun Wang, Ms Rachana Adhikari, and Dr. Li Qian for their involvement in some of the experiments, and Drs. Victor Briz and Pen-Jen Lin for helpful discussions. This work was supported by grant MH101703 to XB and grants NS045260 (PI: Dr. C.M. Gall) and NS057128 to MB. XB is also supported by funds from the Daljit and Elaine Sarkaria Chair.

References

Adelman JP, Maylie J, Sah P. Small-conductance Ca2+-activated K+ channels: form and function. Annu Rev Physiol. 2012; 74:245–269. [PubMed: 21942705]

Baudry M, Bi X. Learning and memory: an emergent property of cell motility. Neurobiol Learn Mem. 2013; 104:64–72. [PubMed: 23707799]

Baudry M, Kramar E, Xu X, Zadran H, Moreno S, Lynch G, Gall C, Bi X. Ampakines promote spine actin polymerization, long-term potentiation, and learning in a mouse model of Angelman syndrome. Neurobiol Dis. 2012; 47:210–215. [PubMed: 22525571]

Benjamin AS, Tullis J. What makes distributed practice effective? Cogn Psychol. 2010; 61:228–247. [PubMed: 20580350]

Bianchetta MJ, Lam TT, Jones SN, Morabito MA. Cyclin-dependent kinase 5 regulates PSD-95 ubiquitination in neurons. J Neurosci. 2011; 31:12029–12035. [PubMed: 21849563]

Bonifacino JS, Cosson P, Klausner RD. Colocalized transmembrane determinants for ER degradation and subunit assembly explain the intracellular fate of TCR chains. Cell. 1990; 63:503–513. [PubMed: 2225064]

Braunewell KH, Manahan-Vaughan D. Long-term depression: a cellular basis for learning? Rev Neurosci. 2001; 12:121–140. [PubMed: 11392454]

Colgin LL, Jia Y, Sabatier JM, Lynch G. Blockade of NMDA receptors enhances spontaneous sharp waves in rat hippocampal slices. Neurosci Lett. 2005; 385:46–51. [PubMed: 15927372]

Colledge M, Snyder EM, Crozier RA, Soderling JA, Jin Y, Langeberg LK, Lu H, Bear MF, Scott JD. Ubiquitination regulates PSD-95 degradation and AMPA receptor surface expression. Neuron. 2003; 40:595–607. [PubMed: 14642282]

Cook EH Jr. Lindgren V, Leventhal BL, Courchesne R, Lincoln A, Shulman C, Lord C, Courchesne E. Autism or atypical autism in maternally but not paternally derived proximal 15q duplication. Am J Hum Genet. 1997; 60:928–934. [PubMed: 9106540]

Deschaux O, Bizot JC, Goyffon M. Apamin improves learning in an object recognition task in rats. Neurosci Lett. 1997; 222:159–162. [PubMed: 9148239]

Dudek SM, Bear MF. Bidirectional long-term modification of synaptic effectiveness in the adult and immature hippocampus. J Neurosci. 1993; 13:2910–2918. [PubMed: 8331379]

Duhovny D, NR.; Wolfson, HJ. Paper presented at: Proceedings of the 2'nd Workshop on Algorithms in Bioinformatics(WABI). Springer Verlag; Rome, Italy: 2002. Efficient Unbound Docking of Rigid Molecules..

Ehlers MD. Activity level controls postsynaptic composition and signaling via the ubiquitin-proteasome system. Nat Neurosci. 2003; 6:231–242. [PubMed: 12577062]

Garcia-Negredo G, Soto D, Llorente J, Morato X, Galenkamp KM, Gomez-Soler M, Fernandez-Duenas V, Watanabe M, Adelman JP, Shigemoto R, et al. Coassembly and Coupling of SK2 Channels and mGlu5 Receptors. J Neurosci. 2014; 34:14793–14802. [PubMed: 25355231]

Guo L, Wang Y. Glutamate stimulates glutamate receptor interacting protein 1 degradation by ubiquitin-proteasome system to regulate surface expression of GluR2. Neuroscience. 2007; 145:100–109. [PubMed: 17207582]

Hammond RS, Bond CT, Strassmaier T, Ngo-Anh TJ, Adelman JP, Maylie J, Stackman RW. Small-conductance Ca2+-activated K+ channel type 2 (SK2) modulates hippocampal learning, memory, and synaptic plasticity. J Neurosci. 2006; 26:1844–1853. [PubMed: 16467533]

Huang L, Kinnucan E, Wang G, Beaudenon S, Howley PM, Huibregtse JM, Pavletich NP. Structure of an E6AP-UbcH7 complex: insights into ubiquitination by the E2-E3 enzyme cascade. Science. 1999; 286:1321–1326. [PubMed: 10558980]

Huibregtse JM, Scheffner M, Beaudenon S, Howley PM. A family of proteins structurally and functionally related to the E6-AP ubiquitin-protein ligase. Proc Natl Acad Sci U S A. 1995; 92:2563–2567. [PubMed: 7708685]

Jiang YH, Armstrong D, Albrecht U, Atkins CM, Noebels JL, Eichele G, Sweatt JD, Beaudet AL. Mutation of the Angelman ubiquitin ligase in mice causes increased cytoplasmic p53 and deficits of contextual learning and long-term potentiation. Neuron. 1998; 21:799–811. [PubMed: 9808466]

Jurd R, Thornton C, Wang J, Luong K, Phamluong K, Kharazia V, Gibb SL, Ron D. Mind bomb-2 is an E3 ligase that ubiquitinates the N-methyl-D-aspartate receptor NR2B subunit in a phosphorylation-dependent manner. J Biol Chem. 2008; 283:301–310. [PubMed: 17962190]

Kim JY, Kim MK, Kang GB, Park CS, Eom SH. Crystal structure of the leucine zipper domain of small-conductance Ca2+-activated K+ (SK(Ca)) channel from Rattus norvegicus. Proteins. 2008; 70:568–571. [PubMed: 17910055]

Komander D, Reyes-Turcu F, Licchesi JD, Odenwaelder P, Wilkinson KD, Barford D. Molecular discrimination of structurally equivalent Lys 63-linked and linear polyubiquitin chains. EMBO Reports. 2009; 10:466–473. [PubMed: 19373254]

Kramar EA, Babayan AH, Gavin CF, Cox CD, Jafari M, Gall CM, Rumbaugh G, Lynch G. Synaptic evidence for the efficacy of spaced learning. Proc Natl Acad Sci U S A. 2012; 109:5121–5126. [PubMed: 22411798]

Kumar S, Talis AL, Howley PM. Identification of HHR23A as a substrate for E6-associated protein-mediated ubiquitination. J Biol Chem. 1999; 274:18785–18792. [PubMed: 10373495]

Lin A, Hou Q, Jarzylo L, Amato S, Gilbert J, Shang F, Man HY. Nedd4-mediated AMPA receptor ubiquitination regulates receptor turnover and trafficking. J Neurochem. 2011; 119:27–39. [PubMed: 21338354]

Lin AW, Man HY. Ubiquitination of neurotransmitter receptors and postsynaptic scaffolding proteins. Neural Plast. 2013; 2013:432057. [PubMed: 23431475]

Lin MT, Lujan R, Watanabe M, Adelman JP, Maylie J. SK2 channel plasticity contributes to LTP at Schaffer collateral-CA1 synapses. Nat Neurosci. 2008; 11:170–177. [PubMed: 18204442]

Lussier MP, Nasu-Nishimura Y, Roche KW. Activity-dependent ubiquitination of the AMPA receptor subunit GluA2. J Neurosci. 2011; 31:3077–3081. [PubMed: 21414928]

Lynch G, Kramar EA, Babayan AH, Rumbaugh G, Gall CM. Differences between synaptic plasticity thresholds result in new timing rules for maximizing long-term potentiation. Neuropharmacology. 2013; 64:27–36. [PubMed: 22820276]

Lynch G, Rex CS, Chen LY, Gall CM. The substrates of memory: defects, treatments, and enhancement. Eur J Pharmacol. 2008; 585:2–13. [PubMed: 18374328]

Mabb AM, Ehlers MD. Ubiquitination in postsynaptic function and plasticity. Annu Rev Cell Dev Biol. 2010; 26:179–210. [PubMed: 20604708]

Malenka RC, Bear MF. LTP and LTD: an embarrassment of riches. Neuron. 2004; 44:5–21. [PubMed: 15450156]

McKay BM, Oh MM, Galvez R, Burgdorf J, Kroes RA, Weiss C, Adelman JP, Moskal JR, Disterhoft JF. Increasing SK2 channel activity impairs associative learning. J Neurophysiol. 2012; 108:863–870. [PubMed: 22552186]

Mu Y, Otsuka T, Horton AC, Scott DB, Ehlers MD. Activity-dependent mRNA splicing controls ER export and synaptic delivery of NMDA receptors. Neuron. 2003; 40:581–594. [PubMed: 14642281]

Ngo-Anh TJ, Bloodgood BL, Lin M, Sabatini BL, Maylie J, Adelman JP. SK channels and NMDA receptors form a Ca2+-mediated feedback loop in dendritic spines. Nat Neurosci. 2005; 8:642–649. [PubMed: 15852011]

Ohtsuki G, Piochon C, Adelman JP, Hansel C. SK2 channel modulation contributes to compartment-specific dendritic plasticity in cerebellar Purkinje cells. Neuron. 2012; 75:108–120. [PubMed: 22794265]

Patrick GN, Bingol B, Weld HA, Schuman EM. Ubiquitin-mediated proteasome activity is required for agonist-induced endocytosis of GluRs. Curr Biol. 2003; 13:2073–2081. [PubMed: 14653997]

Pignatelli M, Piccinin S, Molinaro G, Di Menna L, Riozzi B, Cannella M, Motolese M, Vetere G, Catania MV, Battaglia G, et al. Changes in mGlu5 receptor-dependent synaptic plasticity and coupling to homer proteins in the hippocampus of Ube3A hemizygous mice modeling angelman syndrome. J Neurosci. 2014; 34:4558–4566. [PubMed: 24672001]

Poschel B, Stanton PK. Comparison of cellular mechanisms of long-term depression of synaptic strength at perforant path-granule cell and Schaffer collateral-CA1 synapses. Prog Brain Res. 2007; 163:473–500. [PubMed: 17765734]

Qin Q, Baudry M, Liao G, Noniyev A, Galeano J, Bi X. A novel function for p53: regulation of growth cone motility through interaction with Rho kinase. J Neurosci. 2009; 29:5183–5192. [PubMed: 19386914]

Rapoport M, Lorberboum-Galski H. TAT-based drug delivery system--new directions in protein delivery for new hopes? Expert Opin Drug Deliv. 2009; 6:453–463. [PubMed: 19413454]

Ren Y, Barnwell LF, Alexander JC, Lubin FD, Adelman JP, Pfaffinger PJ, Schrader LA, Anderson AE. Regulation of surface localization of the small conductance Ca2+-activated potassium channel, Sk2, through direct phosphorylation by cAMP-dependent protein kinase. J Biol Chem. 2006; 281:11769–11779. [PubMed: 16513649]

Roche KW, Standley S, McCallum J, Dune Ly C, Ehlers MD, Wenthold RJ. Molecular determinants of NMDA receptor internalization. Nat Neurosci. 2001; 4:794–802. [PubMed: 11477425]

Schneidman-Duhovny D, Inbar Y, Nussinov R, Wolfson HJ. PatchDock and SymmDock: servers for rigid and symmetric docking. Nucleic Acids Res. 2005; 33:W363–367. [PubMed: 15980490]

Smith KE, Gibson ES, Dell'Acqua ML. cAMP-dependent protein kinase postsynaptic localization regulated by NMDA receptor activation through translocation of an A-kinase anchoring protein scaffold protein. J Neurosci. 2006; 26:2391–2402. [PubMed: 16510716]

Stackman RW, Hammond RS, Linardatos E, Gerlach A, Maylie J, Adelman JP, Tzounopoulos T. Small conductance Ca2+-activated K+ channels modulate synaptic plasticity and memory encoding. J Neurosci. 2002; 22:10163–10171. [PubMed: 12451117]

Standley S, Roche KW, McCallum J, Sans N, Wenthold RJ. PDZ domain suppression of an ER retention signal in NMDA receptor NR1 splice variants. Neuron. 2000; 28:887–898. [PubMed: 11163274]

Sun J, Liu Y, Moreno S, Baudry M, Bi X. Imbalanced mechanistic target of rapamycin c1 and c2 activity in the cerebellum of angelman syndrome mice impairs motor function. J Neurosci. 2015; 35:4706–4718. [PubMed: 25788687]

van Woerden GM, Harris KD, Hojjati MR, Gustin RM, Qiu S, de Avila Freire R, Jiang YH, Elgersma Y, Weeber EJ. Rescue of neurological deficits in a mouse model for Angelman syndrome by reduction of alphaCaMKII inhibitory phosphorylation. Nat Neurosci. 2007; 10:280–282. [PubMed: 17259980]

Vick, K.A.t.; Guidi, M.; Stackman, RW, Jr.. In vivo pharmacological manipulation of small conductance Ca(2+)-activated K(+) channels influences motor behavior, object memory and fear conditioning. Neuropharmacology. 2010; 58:650–659. [PubMed: 19944112]

Wang Y, Zhu G, Briz V, Hsu YT, Bi X, Baudry M. A molecular brake controls the magnitude of long-term potentiation. Nat Commun. 2014; 5:3051. [PubMed: 24394804]

Williams CA, Zori RT, Stone JW, Gray BA, Cantu ES, Ostrer H. Maternal origin of 15q11-13 deletions in Angelman syndrome suggests a role for genomic imprinting. Am J Med Genet. 1990; 35:350–353. [PubMed: 2309781]

Xirodimas D, Saville MK, Edling C, Lane DP, Lain S. Different effects of p14ARF on the levels of ubiquitinated p53 and Mdm2 in vivo. Oncogene. 2001; 20:4972–4983. [PubMed: 11526482]

Xu W, Wong TP, Chery N, Gaertner T, Wang YT, Baudry M. Calpain-mediated mGluR1alpha truncation: a key step in excitotoxicity. Neuron. 2007; 53:399–412. [PubMed: 17270736]

Yashiro K, Riday TT, Condon KH, Roberts AC, Bernardo DR, Prakash R, Weinberg RJ, Ehlers MD, Philpot BD. Ube3a is required for experience-dependent maturation of the neocortex. Nat Neurosci. 2009; 12:777–783. [PubMed: 19430469]

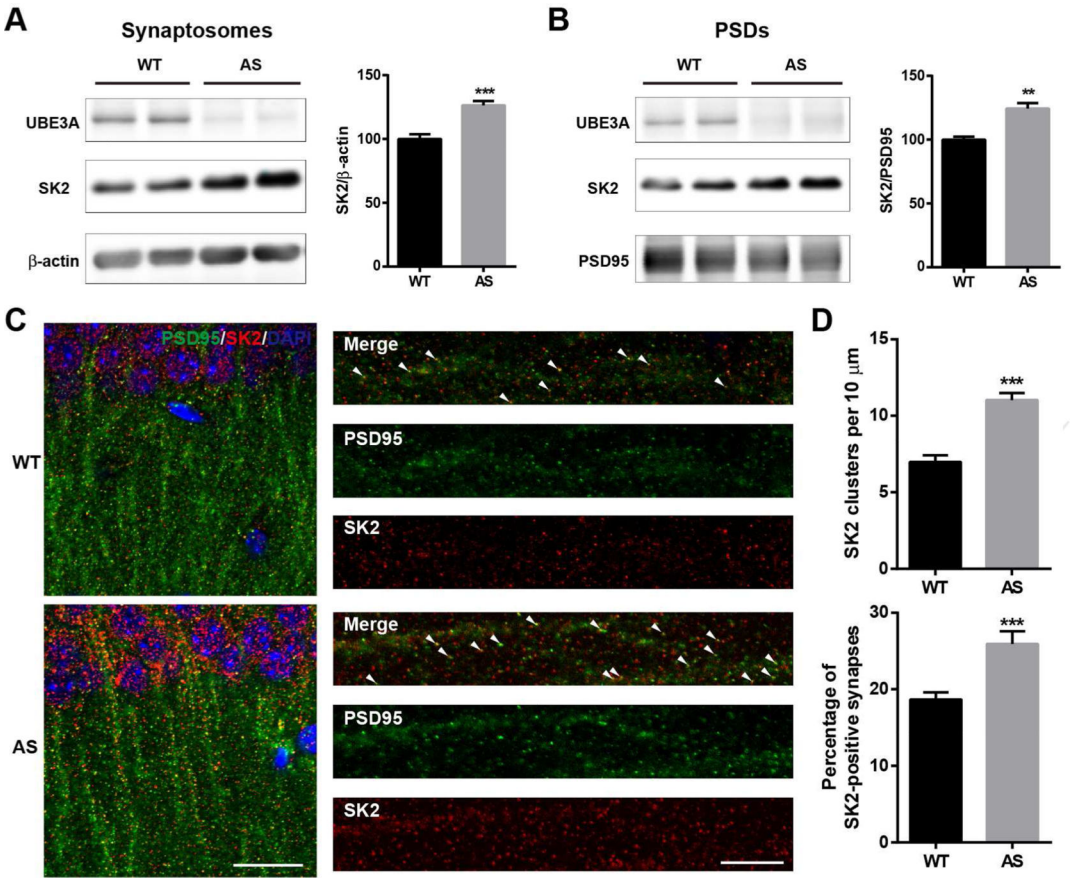

Figure 1. SK2 expression in hippocampus of AS and WT mice

(A,B) Western blot analysis of SK2 levels in (A) crude synaptosomal fractions (P2) and (B) PSD fractions (P3). Optical densities of the SK2 band are normalized to those of β-actin or PSD-95. Data are expressed as % of values in WT mice and shown as means ± S.E.M of 9-10 (in a) or 3 mice (in b) from at least 3 litters, ***p <0.001 (unpaired t-test) and **p < 0.01 (unpaired t-test).

(C) Localization of synaptic SK2 in AS mice. Representative images of CA1 pyramidal neurons stained with anti-SK2 (red) and -PSD95 (green) antibodies. Arrowheads indicate clearly co-localized puncta. Left panel, scale bar = 20 μm. Right panel, scale bar = 10 μm.

(D) Quantitative analysis of the number of SK2-immunoreactive puncta and percentage of SK2 and PSD95 dually stained puncta/synapses in hippocampal CA1 region. N = 18-24 regions of interest from at least 9 slices from at least 3 mice per group (unpaired t-test, ***p<0.001). See also Figure S1.

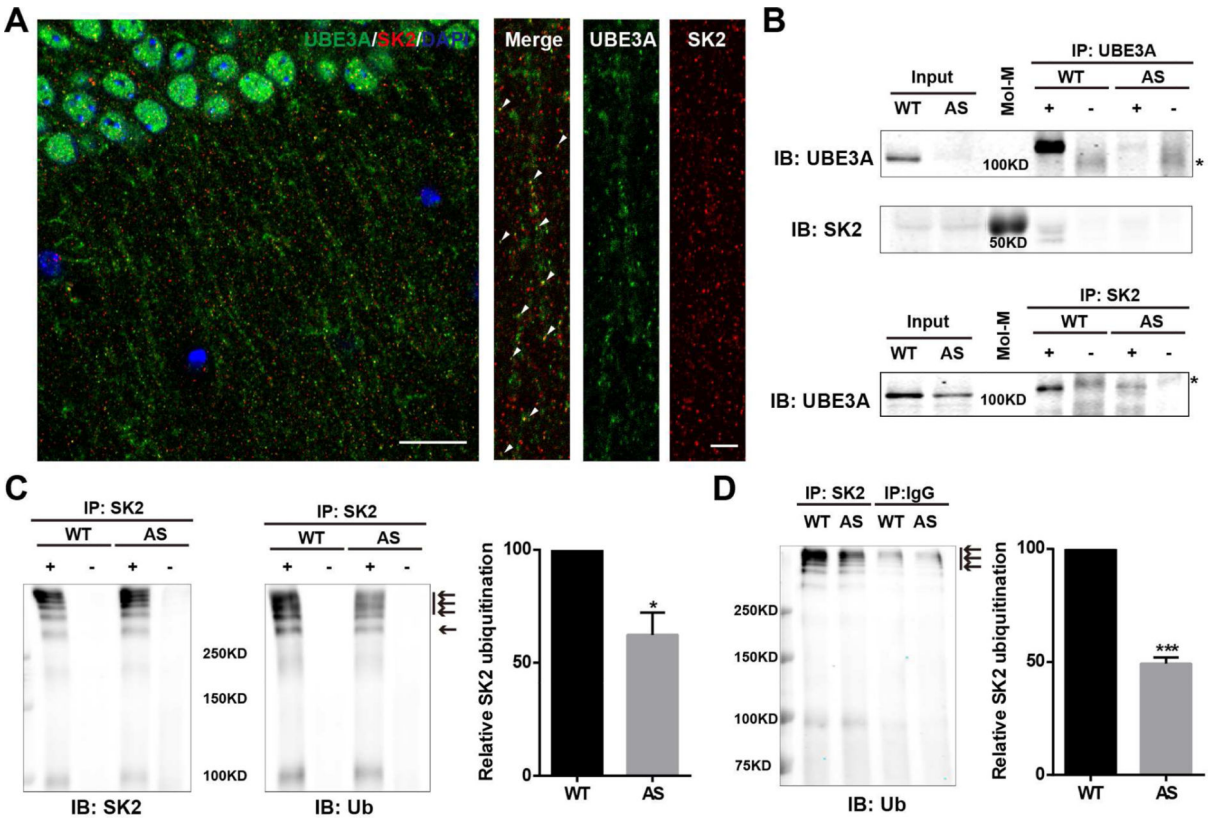

Figure 2. Interactions between UBE3A and SK2 and SK2 ubiquitination in hippocampal membrane fractions from WT and AS mice

(A) Localization of UBE3A (green) and SK2 (red) in dendritic spines along apical dendrites of CA1 pyramidal neurons from a WT mouse (arrowheads indicate clear co-localization). Left panel, scale bar=20 μm. Right panel, scale bar=5 μm.

(B) Interactions between UBE3A and SK2 in hippocampal P2 fractions. Upper panel, Western blot analysis with anti-UBE3A and -SK2 antibodies of immunoprecipitation performed with anti-UBE3A antibodies (+) or control IgG (−). SK2 is clearly co-immunoprecipitated with UBE3A in WT mice. Lower panel, immunoprecipitation was performed with anti-SK2 antibodies and Western blots were labelled with anti-UBE3A antibodies. UBE3A is co-immunoprecipitated with SK2 in WT mice and in AS mice albeit with reduced amount. * indicates non-specific bands in control IgG groups. Mol-M, molecular weight marker.

(C) Immunoprecipitation was performed with anti-SK2 antibodies and Western blots were labelled with anti-SK2 and -ubiquitin (Ub) antibodies. Arrows indicate ubiquitinated SK2 and/or SK2-associated proteins. Right panel, quantification of the relative abundance of ubiquitinated SK2 and/or SK2-associated proteins in hippocampus of WT and AS mice (means ± SEM, * $p < 0.05$, as compared to WT mice, n=3, Student's t test).

(D) Immunoprecipitation under denaturing conditions was performed with anti-SK2 antibodies or control IgG and Western blots were labelled with anti-ubiquitin antibodies. Arrows indicate ubiquitinated SK2. Right panel, quantification of the relative abundance of ubiquitinated SK2 in hippocampus of WT and AS mice (means ± SEM, *** $p < 0.001$, as compared to WT mice, n=3, Student's t test). See also Figure S2.

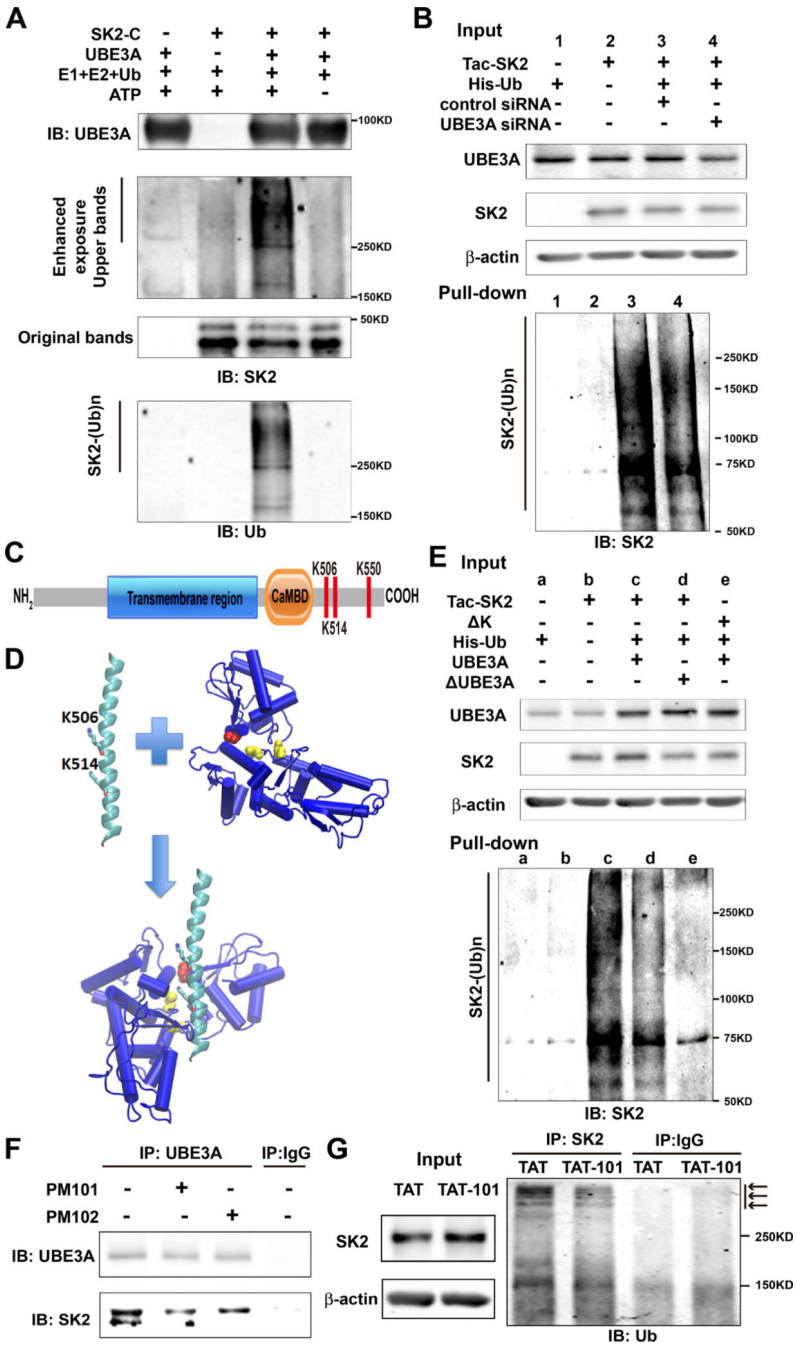

Figure 3. UBE3A ubiquitinates SK2 in the C-terminal domain

(A) *In vitro* ubiquitination of SK2 by recombinant UBE3A. Reaction products were analyzed by Western blot with UBE3A (upper panel), SK2 (middle panel), or ubiquitin (Ub, lower panel) antibodies. Note that ubiquitin and SK2 dually labelled high molecular bands (SK2-(Ub)n) are present only when all reaction elements and ATP were added.

(B) siRNA knock-down of UBE3A in COS-1 cells reduces SK2 ubiquitination. COS-1 cells were incubated with UBE3A siRNA or scrambled control siRNA 24 h before transfection with Tac-SK2 and His-ubiquitin. Twenty-four h later, ubiquitinated proteins were isolated

by Co^{2+}-affinity chromatography. Levels of ubiquitinated Tac-SK2 protein (SK2-(Ub)n, lower panel) were determined by Western blot. Levels of input proteins were also evaluated by Western blot probed with UBE3A, SK2, and β-actin antibodies (Upper panel).

(C) Candidate UBE3A ubiquitination sites (K506/K514/K550) within SK2 C-terminus. CaMBD: calmodulin-binding domain.

(D) Docking of SK2 C-terminal helix (PDB ID 2PNV, chain A 488 to 526) into UBE3A (PDB ID 1D5F). K506 and K514 in the SK2 C-terminal helix are shown in stick. C604 and C737 in the larger N-terminal lobe of UBE3A are shown in yellow balls, and catalytic C820 in the smaller C-terminal lobe is shown in red.

(E) K506A/K514A/K550A (ΔK) mutations in SK2 block UBE3A-mediated SK2 ubiquitination. UBE3A over-expression enhances and K506A/K514A/K550A mutations block SK2 ubiquitination in COS-1 cells. His-tagged ubiquitinated proteins in cells co-transfected with either Tac-SK2 plus UBE3A or ΔUBE3A or ΔK plus UBE3A were precipitated using Talon resin and probed with anti-SK2 antibody (lower panel). Ubiquitinated SK2 are labeled with “SK2-(Ub)n”. Upper panel, input of UBE3A, SK2, and β-actin.

(F) Binding of SK2 with UBE3A is interrupted by PM101 and PM102 peptides. Hippocampal P2 fractions from WT mice were incubated in the presence or absence of PM101 or PM102 (50 μM) peptides followed by immunoprecipitation with either anti-UBE3A antibodies or control IgG. Western blots were performed with anti-UBE3A or anti-SK2 antibodies. Levels of SK2 co-immunoprecipitated with UBE3A were decreased by peptides PM101 or PM102.

(G) Binding of SK2 with UBE3A and its ubiquitination *in vivo* were disrupted by systemic administration of the TAT-101 peptide. WT mice were injected with either control TAT or TAT-101 (i.p. 50 mg/kg) and hippocampi were collected 2 h later for immunoprecipitation and Western blot. Immunoprecipitation under denaturing conditions was performed with anti-SK2 antibodies or control IgG and Western blots were labeled with anti-ubiquitin antibodies (right panel). Arrows indicate ubiquitinated SK2 species. Levels of input proteins were also evaluated by Western blot probed with SK2 and β-actin antibodies (left panel). See also Figure S3.

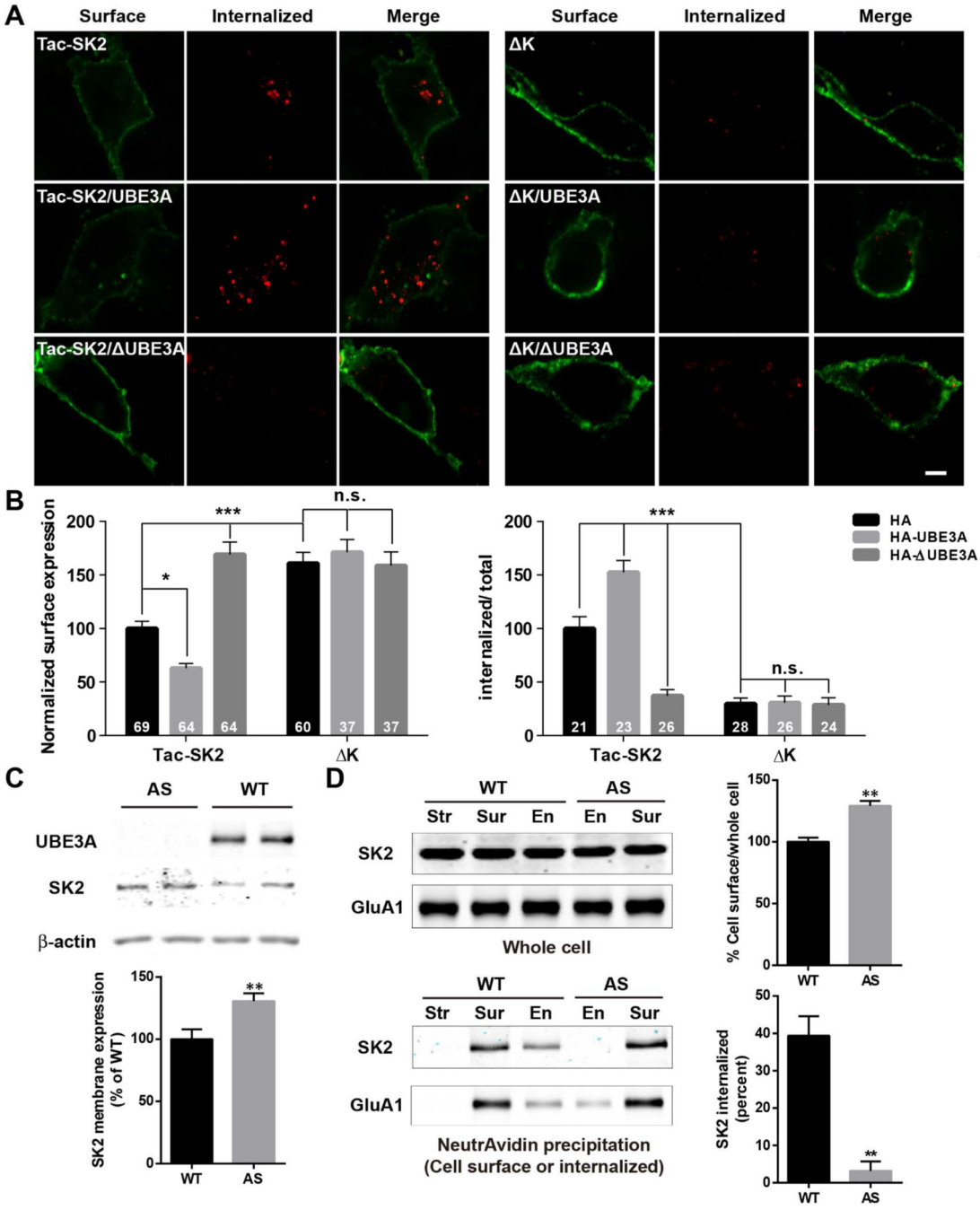

Figure 4. UBE3A regulates SK2 surface expression and endocytosis in COS-1 cells and cultured hippocampal neurons

(A,B) Effects of UBE3A overexpression and K-A mutation on SK2 surface expression and endocytosis. (A) Representative images of internalized (red) or surface-expressed (green) Tac-SK2 (left panels) and ΔK (right panels) in COS-1 cells co-transfected with HA (top panels), HA-UBE3A (middle panels) or HA-ΔUBE3A (bottom panels). Scale bar = 10 μm. (B) Quantitative analysis of images in (A). Data are expressed as means ± S.E.M. *p <0.05, **p <0.01, ***p <0.001, as compared to Tac-SK2/HA (Tac-SK2); two-way ANOVA with

Newman-Keuls post-hoc analysis, N is indicated in each column and from at least 3 independent experiments.

(C-D) Regulation of SK2 membrane expression and internalization by UBE3A in cultured hippocampal neurons. (C) Upper panel: Representative blots of UBE3A, SK2, and β-actin in P2 fractions. Lower panel: Quantitative data (n = 10 – 11 E18 mouse embryos; unpaired Student's t-test, ** $p < 0.01$). (D) Biotinylation assays of SK2 and GluA1 (used as control) endocytosis with hippocampal neurons. Biotinylated SK2 and GluA1 were isolated by NeutrAvidin precipitation and detected by Western blot with SK2 and GluA1 antibodies (lower left panel). Upper left panel, levels of SK2 and GluA1 in whole homogenate (input). Upper right panel, ratio (mean ± S.E.M. of 3 independent experiments) of surface-expressed SK2 over total SK2. Lower right panel, ratio (mean ± S.E.M. of 3 independent experiments) of internalized SK2 over surface-expressed SK2. ** $P < 0.01$, unpaired Student's t-test. Str, samples from stripped dish; Sur, total surface proteins; En, internalized proteins. See also Figure S4.

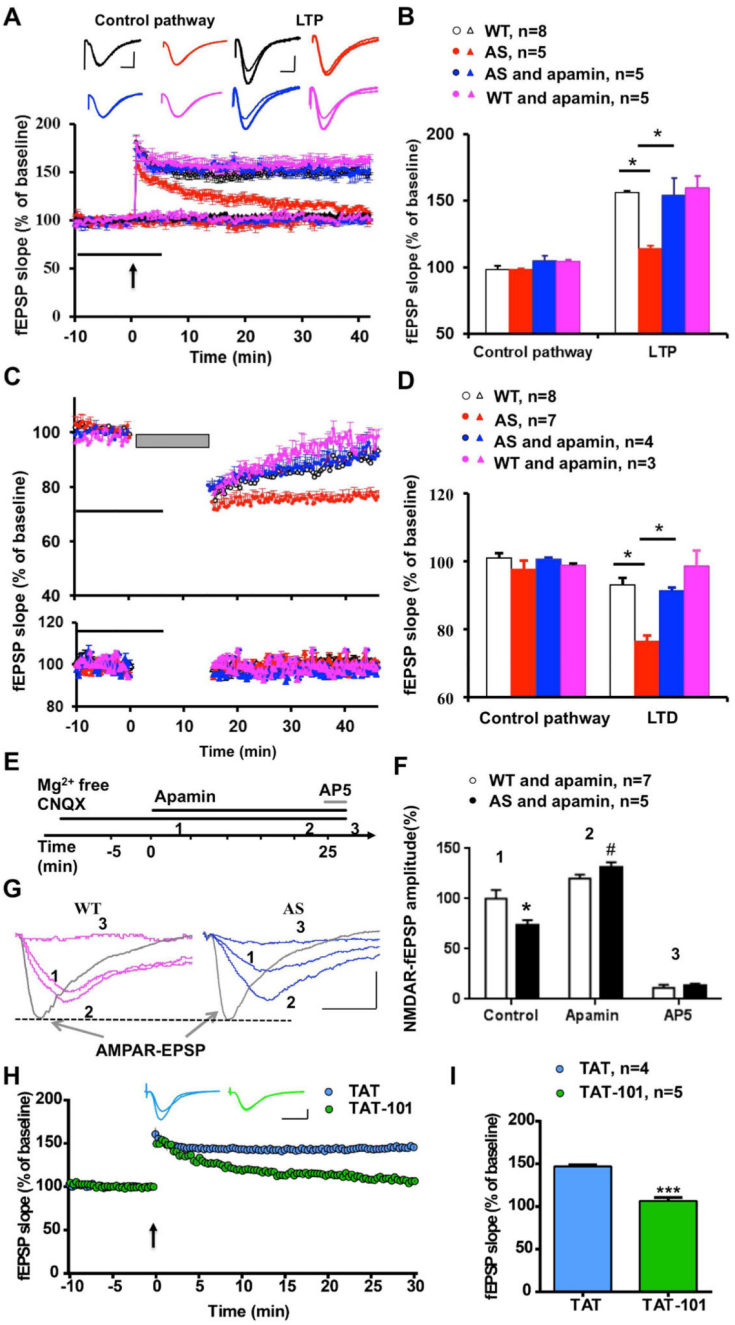

Figure 5. Impairment of NMDA receptor-dependent hippocampal synaptic transmission and activity-dependent synaptic plasticity in hippocampal slices from AS mice

(A) Reversal of LTP impairment in AS mice by SK2 channel blocker, apamin. Slopes of fEPSPs were normalized to the average values recorded during the 10 min baseline. Insert shows representative traces of evoked fEPSPs before and 40 min after TBS (arrow). Scale bar: 0.5 mV/10 ms.

(B) Means ± S.E.M. of fEPSPs (expressed as % of WT control pathway) measured 40 min after TBS in different groups. *p <0.05 (one-way ANOVA followed by Bonferroni test).

(C) LTD in hippocampal slices from AS mice is blocked by apamin. Upper panel: LTD induced by LFS (1 Hz for 15 min). Lower panel: effect of apamin on control pathway.
(D) Means ± S.E.M. of fEPSPs measured 40 min after LFS in different groups. *p <0.05 (one-way ANOVA followed by Bonferroni test).
(E) Protocol and time points used for analysis of NMDAR-mediated synaptic transmission ($_N$fEPSP).
(F,G) Representative traces (G) and quantification of $_N$fEPSPs (F) recorded at the time points indicated in E. Data are expressed as % of values in WT hippocampal slices before apamin treatment (WT control); *p <0.05, as compared to WT control, #p <0.05, as compared to AS control (two-way ANOVA followed by Bonferroni test). Traces of AMPAR fEPSPs indicate that synaptic responses before initiation of $_N$fEPSP recording are similar between AS and WT mice. Scale bar: 0.5 mV/20 ms.
(H) Systemic injection of peptide TAT-101 impaired LTP induction in WT mice. Insert shows representative traces of evoked fEPSPs before and 30 min after TBS (arrow). Scale bar: 0.5 mV/10 ms.
(I) Means ± S.E.M. of fEPSPs measured 30 min after TBS in the two groups. ***p <0.001 (Student's t test). See also Figures S5 and S6.

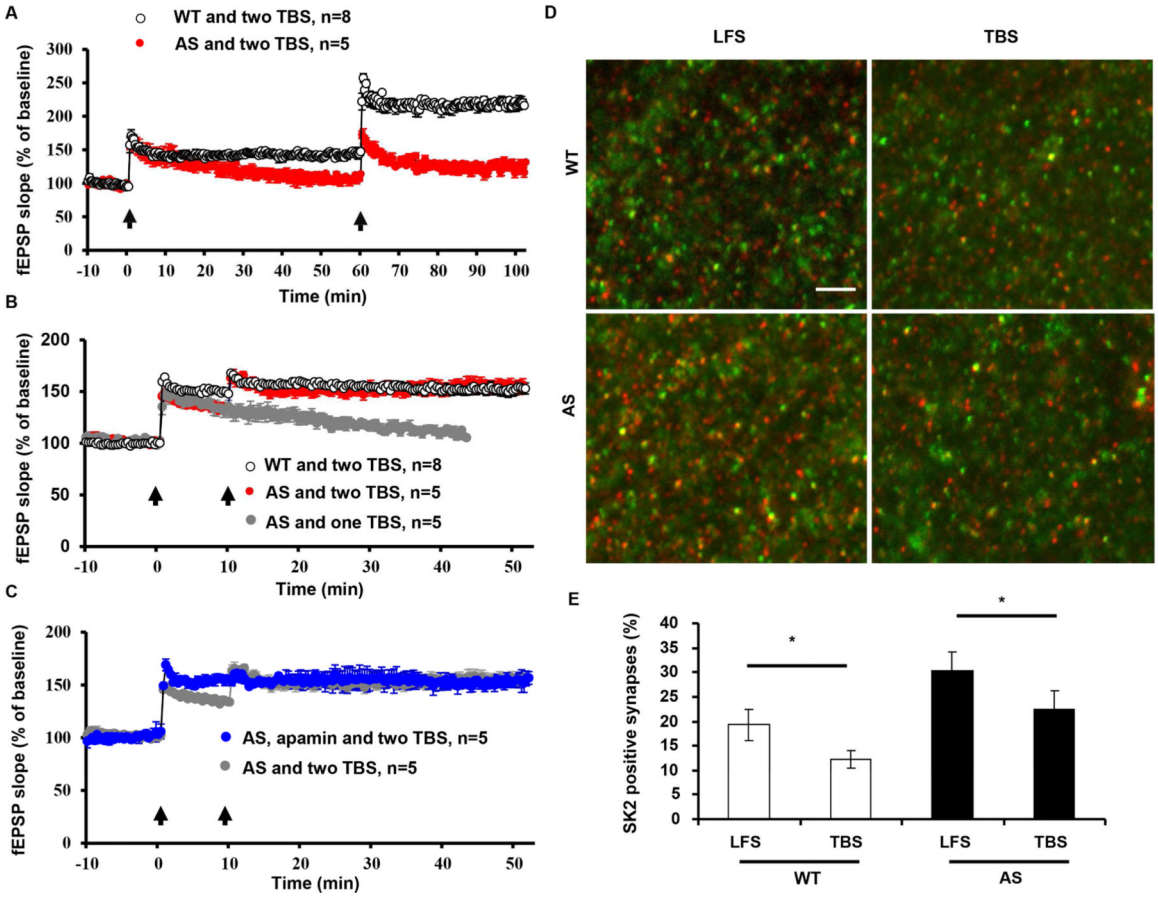

Figure 6. UBE3A deficiency-induced changes in LTP properties

(A) Two TBS (arrows) separated by 60 min could induce further potentiation in hippocampal slices from WT mice, while neither the first or second TBS induced LTP in hippocampal slices from AS mice.

(B) A second TBS(2) applied 10 min after the first TBS(1) did not induce further potentiation in slices from WT mice. However, the same TBS2 was able to induce LTP in hippocampal slices from AS mice.

(C) With apamin pre-application, TBS2 applied 10 min post TBS1 was not able to further enhance LTP in AS mice.

(D) TBS elicited a decrease in the number of SK2-positive synapses in both WT and AS mice. Shown are representative images of SK2 (red) and PSD95 (green) immunostaining in CA1 region of WT and AS mice (Scale bar = 10 μm).

(E) Quantitative results of synapses dually labelled by anti-SK2 and -PSD95 antibodies in different experimental groups (* $p < 0.05$, n = 3 slices from 3 mice/group, one-way ANOVA followed by Bonferroni test). See also Figure S7.

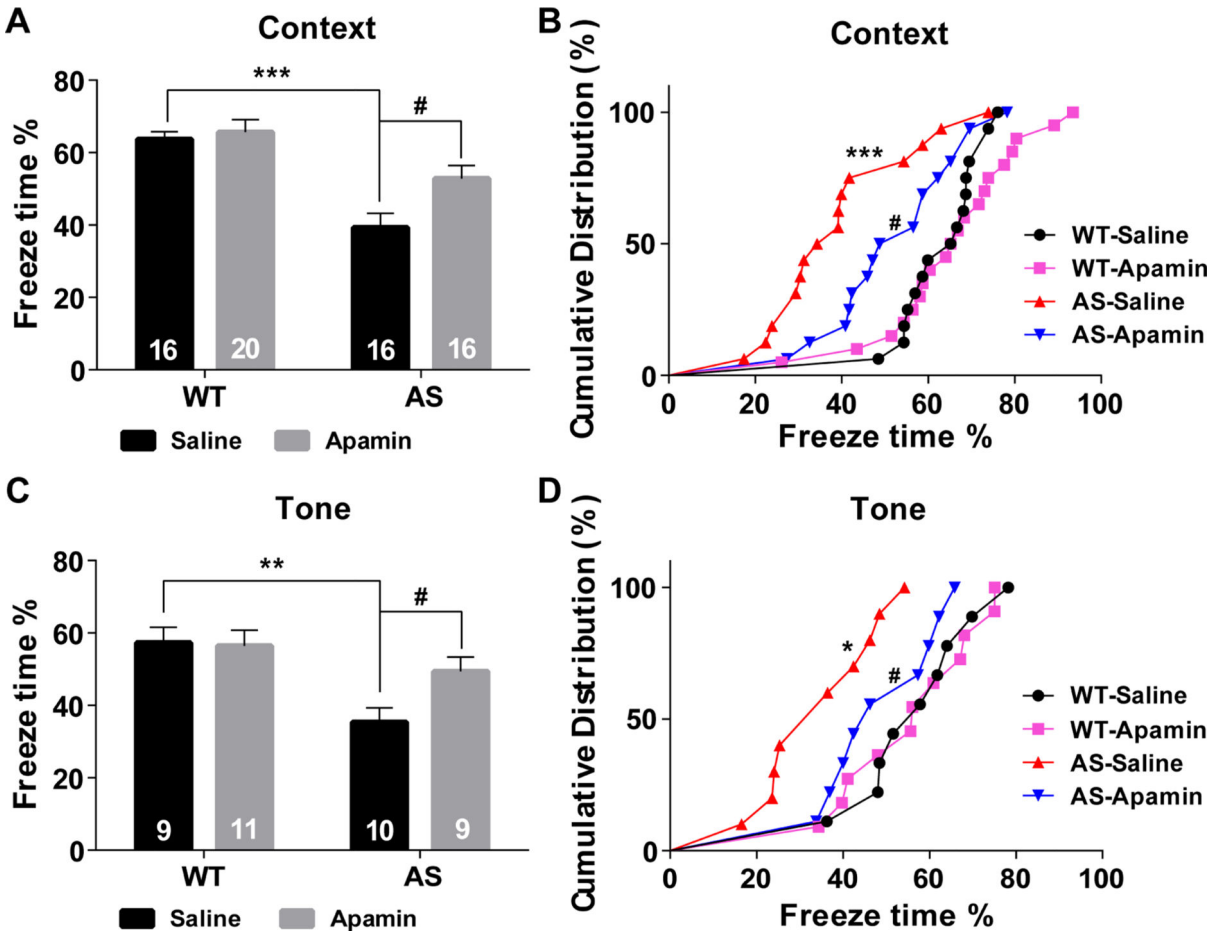

Figure 7. Effects of apamin treatment on fear conditioning in WT and AS mice

(A) % freezing for different experimental groups in context memory (means ± S.E.M. of 16-20 mice; ***p <0.001, as compared to WT controls; #p <0.05, as compared to vehicle-treated AS mice; two-way ANOVA with Newman-Keuls post-hoc analysis).

(B) Cumulative distribution of % freezing in WT and AS mice treated with vehicle or apamin assessed by the Kolmogorov-Smirnov test in context memory (***p <0.001, as compared to WT controls, #p <0.05, as compared to vehicle-treated AS mice).

(C,D) % freezing and cumulative distribution for different experimental groups in tone memory (means ± S.E.M. of 9-11 mice. *p <0.05 and **p <0.01 as compared to WT controls; #p <0.05, as compared to vehicle-treated AS mice). See also Figure S7.